Advancing the State-of-the-Art in Bentonite Barrier Research: Measuring Membrane Behavior and Diffusion at Elevated Temperatures

Sayed Arafat B. Rahman, M.S., S.M.ASCE¹, Kristin M. Sample-Lord, Ph.D., P.E., M.ASCE², Gretchen L. Bohnhoff, Ph.D., P.E., M.ASCE³

¹Graduate Research Assistant, Department of Civil & Environmental Engineering, Villanova University, Villanova, PA 19085; e-mail: srahman6@villanova.edu

²Assistant Professor, Department of Civil & Environmental Engineering, Villanova University, Villanova, PA 19085; e-mail: kristin.sample-lord@villanova.edu

³Associate Professor, Department of Civil & Environmental Engineering, University of Wisconsin-Platteville, Platteville, WI 53818; e-mail: bohnhoffg@uwplatt.edu

ABSTRACT

Sodium bentonite (NaB) is widely used in containment barriers to limit contaminant migration into the environment. The performance of NaB barriers in applications such as landfills, impoundments, and radioactive waste disposal relies on the ability of the NaB to limit liquid and contaminant flux through the barrier for extended durations and under changing environmental conditions. The results of previous studies indicate that NaB may exhibit significant membrane behavior (solute restriction), potentially enhancing the performance of the barrier by reducing both liquid and contaminant flux. However, diffusion and membrane behavior in NaB under variable temperature and chemical conditions is not well understood, largely due to experimental testing challenges. This knowledge gap limits our ability to predict contaminant transport through NaB barriers exposed to elevated temperatures (e.g., high-level radioactive waste disposal). To address this challenge, an innovative testing apparatus was developed for measurement of coupled membrane behavior and diffusion in clays under controlled temperature and chemical conditions. The setup was equipped with heating elements, temperatures sensors, and temperature controllers, along with remote data logging and hydraulic control features. The apparatus design and testing procedures, as well as example results for NaB are presented. Preliminary results indicate that the testing apparatus maintained consistent temperature conditions throughout testing and that membrane behavior decreased with increasing temperature.

INTRODUCTION AND BACKGROUND

Membrane Behavior and Diffusion in Bentonite Barriers

Sodium bentonite (NaB) is widely used in engineered barriers to provide long-term safe containment of chemicals and wastes. Containment applications that rely on NaB-based barriers include, but are not limited to, landfills for municipal or hazardous solid wastes, impoundments for mine tailings or coal combustion residuals, wastewater ponds, waste lagoons, and disposal of radioactive waste. The NaB provides a barrier layer of low hydraulic conductivity (k) that limits liquid flow and contaminant transport into the surrounding environment and groundwater. Most regulatory codes and standards generally stipulate a minimum thickness and maximum k for the

barrier, with focus on controlling leakage and limiting advective flux. The low k, high swell, high sorption capacity, and low diffusion coefficients exhibited by NaB result in engineered barriers that are generally very effective in restricting contaminant mobility for solutions of low ionic strength (Shackelford et al. 2000). Although diffusion is a significant to dominant transport mechanism when advection is restricted (Rowe et al. 1988; Lake and Rowe 2000; Shackelford 2014), consideration of diffusion coefficients is not a regulatory requirement for many NaB barrier applications.

Previous studies have demonstrated NaB may also exhibit significant membrane behavior, i.e., solute (contaminant) restriction, thereby potentially enhancing the performance of the barrier by reducing both liquid and contaminant flux (Shackelford 2013). Membrane behavior refers to the ability of the clay to selectively restrict the passage of dissolved chemical species (solutes). Anion repulsion occurs in the zone of the diffuse double layer due to negative electrical potential. As shown conceptually in Figure 1, anion exclusion occurs when the adjacent clay particles are close enough for the effective diameter of the free solution zone to be less that the diameter of the hydrated anion. When anions are excluded from transporting through the pore space, this leads to similar restriction of cations due to electroneutrality constraints. The thickness of the diffuse double layer of the clay is inversely related to the ionic strength and temperature of the bulk solutions (Francois and Ettahiri 2012). Membrane behavior is quantified by the membrane efficiency coefficient (ω). Values of ω range from 0 for no membrane behavior to 1.0 representing 100 % solute restriction (perfect membrane).

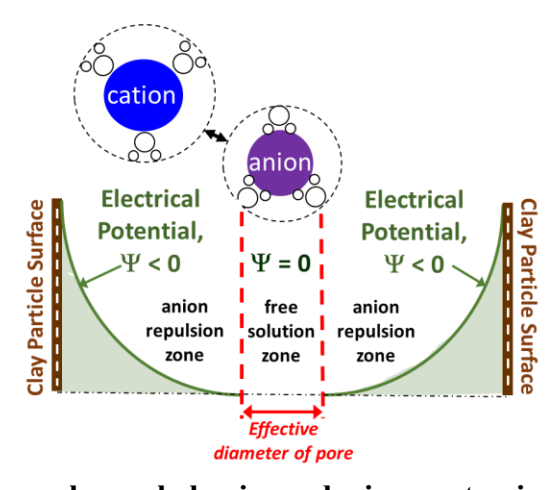


Figure 1. Concept of membrane behavior reducing contaminant flux across barrier.

Relevance of Elevated Temperatures for Bentonite Barriers

Elevated temperature conditions are relevant for many containment applications that utilize NaB, such as high-level radioactive waste (HLRW) disposal and some MSW landfills. For HLRW, geological disposal systems include both the natural geological barrier (e.g., host rock) and an engineered barrier system (EBS). Components of the EBS typically include the canister, buffer, backfill, seals and plugs (OECD 2004). The low *k* and high swelling capacity of compacted NaB makes the material an ideal candidate for use as the buffer between the waste canister and host rock and/or as seals in excavated disposal galleries in the EBS. However, due to radioactive decay of the waste, high temperatures (100-200 °C) are expected to develop adjacent to the waste canisters and persist for thousands of years (Johnson et al. 2002). Thus, effects of elevated

temperatures on the contaminant transport properties of the bentonite barrier are a critical consideration in the design of nuclear waste repositories (Fox et al. 2019).

Although less common, sustained temperatures above 80°C have been reported in some MSW landfills due to biological and chemical reactions (referred to as Elevated Temperature Landfills, ETLFs) (Hao et al. 2017). Assessing and controlling elevated temperatures in landfills is a costly issue, motivating substantial research attention over the last decade (Yafrate and Luettich 2017). Geosynthetic clay liners and compacted clay liners may be exposed to sustained elevated temperatures in addition to complex chemical conditions from waste leachates.

Bentonite exhibits a complex response to changes in temperature, due to the coupled effects of multiple processes (Daniels et al. 2017). Hydraulic conductivity of NaB generally has been shown to increase with increasing temperature (e.g., Pusch et al. 1985; Gray 1993; Cho et al. 1999), but cannot always be explained simply by reductions in water viscosity (e.g., Zihms and Harrington 2015). For NaB exposed to temperatures exceeding 150° C over long durations, cementation by precipitation of SiO₂ and transformation of smectite to illite (illitisation) may lead to reduced swelling, increased k, and increased diffusivity, potentially reducing performance of the barrier (Wersin et al. 2007; Zheng et al. 2015). All of the aforementioned properties also are affected by the pore-water chemistry. Temperature effects on solute diffusion in NaB have been investigated (e.g., Eriksen et al. 1981; Kozaki et al. 1999) but remain even less understood than changes in hydraulic and mechanical properties (Pusch 2001).

To the authors knowledge, no prior studies have experimentally evaluated membrane behavior of NaB under variable temperature and chemical conditions. The thickness of the diffuse double layer in Figure 1 is inversely related to the ionic strength of the bulk solution, but exhibits a much more complex relationship with temperature (T). Increases in T are expected to result in degradation of the double layer (Francois and Ettahiri 2012), yet some experimental studies have shown the opposite trend. The effect of T on the double layer has been shown to also be dependent on the ionic strength of the solution, with increases in ionic strength suppressing the effects of T. Thus, the effect of T on the electrical double layers of clay particles is less evident than the effect of other physico-chemical factors, leading to lack of agreement between theory and experimental results in the clay sciences and engineering (Sokolov and Tchistiakov 1999). The gap in knowledge of the impact of T on membrane behavior of clays is exacerbated by the challenging nature of the experimental measurements, limiting our current ability to predict contaminant transport through NaB barriers at elevated temperatures.

To address this challenge, an innovative testing apparatus was developed for measurement of coupled membrane behavior and diffusion in clays under controlled temperature and chemical conditions. The setup was equipped with heating elements, temperatures sensors, and temperature controllers at both specimen boundaries, along with automated remote hydraulic control features. The apparatus design and testing procedures, as well as example results for two NaB specimens tested at different temperatures, are presented herein.

METHODS

Development of New Testing Apparatus

A state-of-the-art temperature-controlled testing setup was designed and fabricated to simultaneously measure effective diffusion coefficients (D^*) and ω of NaB specimens under different temperature conditions and salt concentrations. The new closed-system apparatus is shown schematically in Figure 2. The use of a closed system allows for several testing advantages

relative to open systems, including easier and more accurate measurement of parameters necessary to quantify membrane behavior, easier control of boundary conditions, and linear concentration profiles across the specimen at steady state diffusion, which allow for less complex analyses than required in open systems with nonlinear profiles (Shackelford 2013). The design of the apparatus was based upon test systems originally published by Malusis et al. (2001), with the primary advancements being the addition of automated temperature and hydraulic controls.

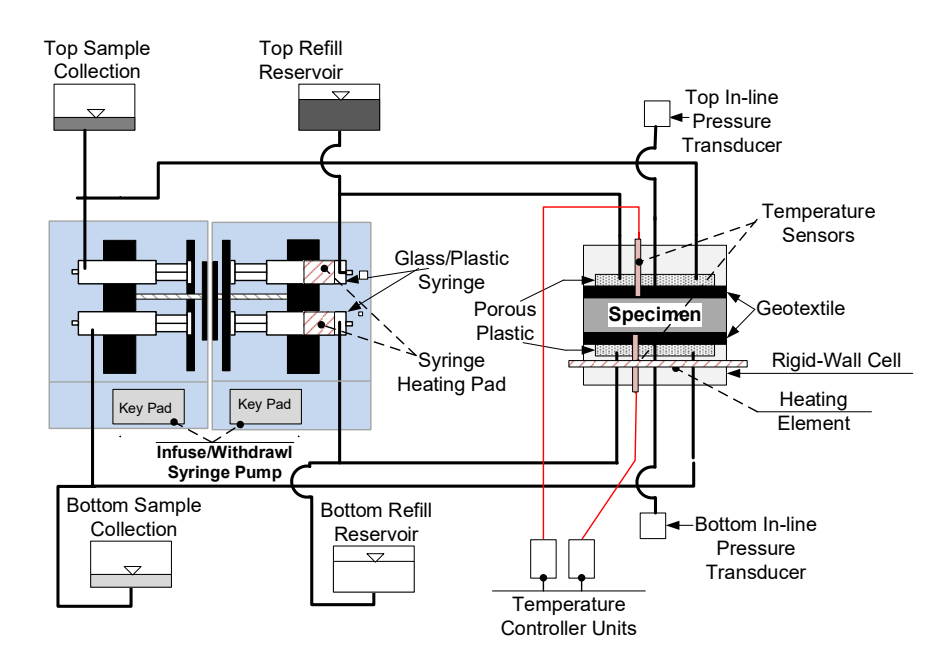


Figure 2. Temperature-controlled membrane behavior and diffusion testing apparatus.

The rigid-wall cell was equipped with 6-inch-long general-purpose platinum Resistance Temperature Detector (RTD) probes (Omega Engineering Inc, Model PRTF-10-2-100, Norwalk, CT) to measure temperatures at each specimen boundary. The temperature probes were connected to a separate proportional-integral-derivative (PID) temperature controller unit (Inkbird, Model ITC-106RL) to regulate the heating of the specimen to a set temperature within the rigid-wall cell via a heating element (Model HTC451005, BriskHeat, Columbus, OH) wrapped around the cell. The cell was housed inside a partially sealed compartment (small greenhouse; Figure 3) to reduce the amount of heat loss and associated disturbance to the regulated temperature of the specimen. The test setup is also monitored using a Wi-Fi camera (Amcrest Industries LLC, Houston, TX).

To measure ω and D^* , a constant concentration gradient is applied across the specimen. Salt solutions and de-ionized water (DIW) are circulated separately across the top and bottom boundaries of the specimen, respectively, using a six channel programmable syringe pump (New Era Pump Systems, Model NE-1600, Farmingdale, NY) with two syringes on each pump. The two pumps (named as infusion and withdrawal pump based on their sole function in the system) were operated in reciprocating mode to ensure the closed system. While one pump infuses the liquids through the top and bottom boundary of the specimen within the rigid-wall cell at a constant rate through porous plastic disks adjacent to the specimen, the other pump withdraws the liquids at the same rate from the specimen boundaries. The solutions circulating through the porous plastic disks at each boundary of the specimen establish the concentration difference (ΔC) across the specimen. If the specimen acts as a semipermeable membrane, then a chemico-osmotic pressure difference

 (ΔP) will develop across the length of the specimen (L) due to the applied ΔC . The value of ΔP is determined from pressure transducer measurements at each boundary (in this study: Cole-Parmer, Model Ashcroft DG25, Vernon Hills, IL).

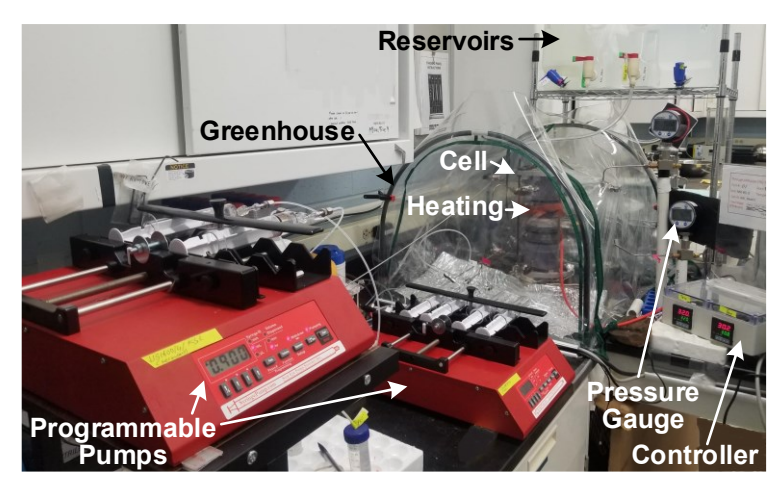


Figure 3. Photograph of temperature-controlled apparatus.

After circulating across the specimen boundaries, the outflows enter the withdrawal syringes and then are automatically dispensed into 50-mL collection vials via dual check valves. The infusion syringes are automatically refilled every two days from the top and bottom reservoirs shown in Figure 2. Collected outflow samples then are analyzed for chloride (Cl⁻) concentration, electrical conductivity (*EC*), and pH via Orion Versa Star benchtop meter (Ross Ultra Triode and DuraProbe Conductivity Cell, Thermo Scientific Orion, Waltham, MA) with Chloride ion selective electrode (ISE, Orion 9617BNWP Chloride Combinate Electrode), Conductivity Cell (Orion 013005MD Conductivity Cell) and pH probe (Orion 8157BNUMD ROSS Ultra pH/ATC Triode). Randomly selected samples were also analyzed with a Systea direct reading discrete analyzer (Model Easychem 200) to confirm Cl⁻ concentrations measured with the ISE probe.

The testing is performed in stages, where the first stage consists of circulating DIW across both top and bottom boundaries to establish the baseline value of ΔP . Once steady baseline pressures are established, the DIW at the top boundary is switched to an electrolyte solution (e.g., KCl), inducing a buildup of ΔP , i.e., if membrane behavior exists in the specimen. After both steady-state ΔP and diffusion (discussed subsequently) are established, the ΔC may be increased via circulation of a higher concentration solution, beginning a new stage of the same test. The total duration required to complete each concentration stage typically ranges from three to five weeks depending on responses of the specimen to the thermo-hydro-chemical changes in the system.

Analysis

For the described testing system, ω is calculated using the following relationship:

$$\omega = \frac{\Delta P}{\Delta \pi} \tag{1}$$

where $\Delta\pi$ is the theoretical maximum chemico-osmotic pressure difference across an ideal semipermeable membrane. The value of where $\Delta\pi$ is calculated based on the van't Hoff expression:

$$\Delta \pi = \nu R T \Delta C \tag{2}$$

where v is the number of ions from one molecule of salt (e.g., v = 2 for KCl), R is the universal gas constant (8.314 J mol⁻¹K⁻¹), and T is the absolute temperature in Kelvin. The value of ΔC is the concentration difference across the specimen and is calculated as the difference between the average concentrations at the top and bottom boundaries.

Maintaining approximately constant concentrations at each boundary via the throughdiffusion testing method also allows for calculation of the D^* using the steady-state analysis method. Details of the analysis method are provided in Shackelford (1991) and are summarized herein for convenience. Based on the concentration of the outflow samples collected from the bottom boundary of the specimen, the concentration of solutes diffusing through the specimen are converted to the area-normalized cumulative mass (Q_t) , as follows:

$$Q_t = \frac{1}{A} \sum_{i=1}^{N_S} \Delta m_i \tag{3}$$

where A is the cross-sectional area of the specimen and Δm_i is the incremental mass of the solute collected over time increment Δt (Δm_i = concentration of outflow sample x volume of outflow sample collected over Δt). Values of Q_t are then plotted versus elapsed time. During the initial phases of the test stage, the Q_t -vs.-t plot is nonlinear during transient diffusion conditions. Once steady-state diffusion is reached, Q_t -vs.-t becomes linear, and a linear regression can be fit to the end of the data set to determine D^* as follows (Shackelford 1991):

$$D^* = \left(\frac{\Delta Q_t}{\Delta t}\right) \left(\frac{L}{n w_A \Delta C}\right) \tag{4}$$

where $\Delta Q_l/\Delta t$ represents the slope of the linear regression, L is the thickness of the specimen thickness, n is the porosity, w_A is the atomic weight of the diffusing solute (35.45 g/mol for Cl⁻), and ΔC is the molar concentration difference of the solute across the specimen.

EXAMPLE RESULTS

Example results are presented for coupled membrane behavior and diffusion testing using the previously described testing apparatus for two similar NaB specimens for the same salt concentration (10 mM KCl), but tested at two different temperatures (23 °C and 50 °C).

Specimen Preparation and Liquids

The NaB used in the test program was MX-80 (CETCO). The measured swell index and liquid limit with DIW at room temperature (23 °C) were 23.5 mL/2g and 336 %, respectively. Specimens were prepared in the rigid-wall cell with the thicknesses and porosities summarized in Table 1 for the two tests. To allow for comparison with the membrane behavior literature, KCl solution was used as the salt solution circulated at the top boundary. The solutions used in the example test included DIW (Electrical Conductivity, EC, at 25 °C = 0.17 mS/m) and 10 mM KCl solution (EC = 144 mS/m).

Boundary Temperatures

Throughout the membrane behavior and diffusion testing, constant controlled temperatures were maintained at each boundary of the specimen. The temperatures monitored with the temperature sensors throughout the 10 mM KCl test stage are shown in Figure 4. As demonstrated in the plots, temperatures were well controlled (minimal variability) and there was no observable temperature gradient between the top and bottom boundaries (i.e., the data series plotted on top of each other).

Table 1. Properties of the bentonite specimens in the example tests.

| Prepared Specimen | Temperature for Membrane Behavior & Diffusion Test | |
|------------------------|--|-------|
| | 23° C | 50° C |
| Thickness, L (cm) | 0.71 | 0.72 |
| Porosity, <i>n</i> (-) | 0.73 | 0.73 |

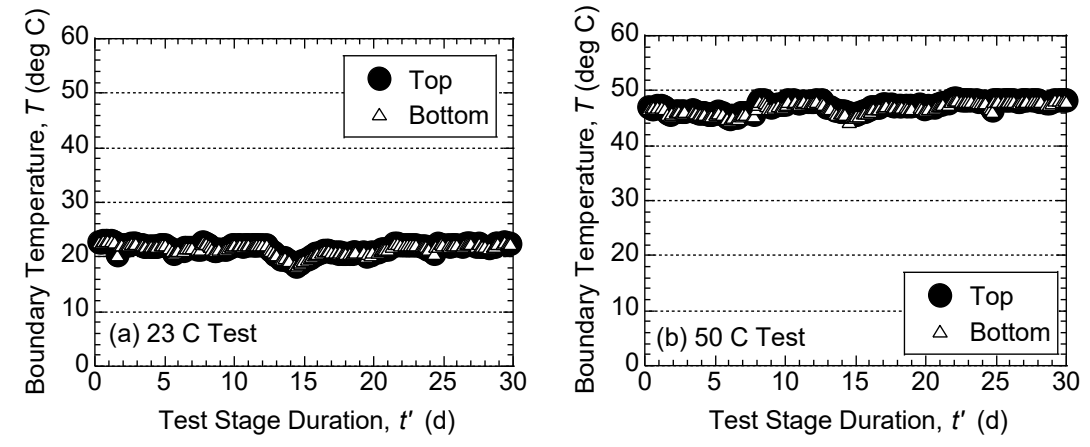


Figure 4. Measured temperatures at the top and bottom boundaries of specimen during the membrane behavior and diffusion testing performed at: (a) 23° C; and (b) 50° C.

Membrane Efficiency and Diffusion Coefficients

Prior to circulation of salt solution, DIW was circulated at each boundary of the specimen to determine the baseline differential pressure (ΔP_o), consistent with procedures described in Malusis et al. (2001). Values of ΔP_o for the 23 °C and 50 °C test were 4.71 and 6.47 kPa, respectively. The differential pressures measured across the specimens during the 10 mM KCl stage after correcting for ΔP_o (ΔP_e) are shown in Figure 5. Diffusion coefficients for chloride were determined from plots of Q_t vs. t as described previously and shown in Figure 6.

The drops in the ΔP_e values in the plots in Figure 5 are due to the pump reversals/restarts as part of the testing procedure and are typically ignored in the analysis of membrane behavior (e.g., Kang and Shackelford 2010). The peaks in ΔP_e for each circulation cycle are used to determine ω . From Figure 5, there is a clear impact of temperature on the measured value of ΔP_e . For the test performed at room temperature (23 °C), the steady-state ΔP_e value averaged 24.13 kPa, whereas the test performed at 50 °C had a much lower average ΔP_e of 8.27 kPa. The lower ΔP_e at higher temperature (T) directly corresponds to lower ω , based on Equation 1. As summarized in Table 3, the values of ω for the 23 °C and 50 °C test were 58.5 % and 19.1 %, respectively.

The values of ω for the test conducted at room temperature are similar to results reported in literature (e.g., Malusis et al. 2001; Kang and Shackelford 2010; Dominijanni et al 2013). For example, Malusis et al. (2001) reported ω values that ranged from 38 % to 51 % for GCLs tested under similar concentrations of KCl (8.7 mM). However, the elevated temperature test ω is much lower than ω that have been reported in literature for NaB at room temperature (19.1 % versus 38 %, respectively). Increases in T are expected to result in degradation of the diffuse double layer (Francois and Ettahiri 2012), likely contributing to the observed decrease in ω with increasing T. Further study is required to elucidate mechanisms controlling changes in ω with T, due to the complex response of NaB to high T as described previously.

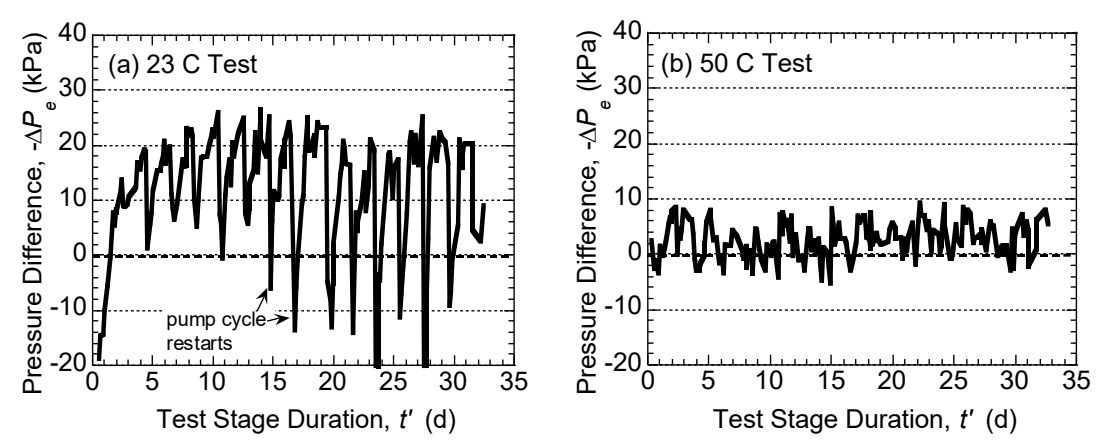


Figure 5. Measured differential pressures across the specimens at: (a) 23° C; (b) 50° C.

Table 3. Results for 10 mM KCl concentration stage for two different temperatures.

| Test Temperature (° C) | Membrane Efficiency Coefficient, ω (%) | Effective Diffusion Coefficient for Chloride, $D^* (x 10^{-10} \text{ m}^2/\text{s})$ |
|------------------------|---|---|
| 23 | 44.5 | 1.60 |
| 50 | 14.2 | 1.63 |

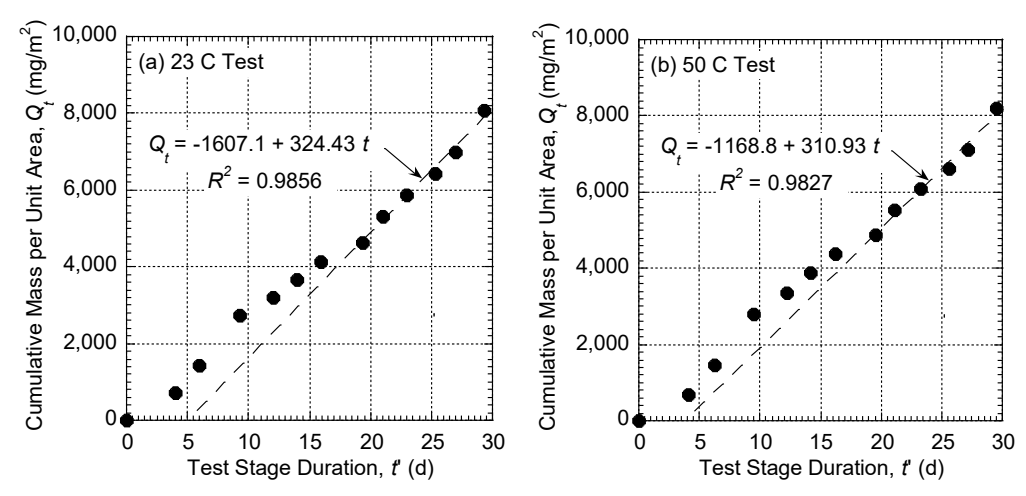


Figure 6. Cumulative diffused mass per specimen area for tests at: (a) 23° C; (b) 50° C. (Linear regression includes the last six data points)

The D^* values were similar at 1.60 x 10^{-10} m²/s for the test performed at 23° C and 1.63 x 10^{-10} m²/s for the test performed at 50° C. Although elevated-temperature diffusion studies in the literature generally report increasing D^* with increasing T, most of the studies are for temperatures exceeding 80 °C, and thus are difficult to compare with the results in Table 3. The D^* values in Table 3 are higher than those reported in the literature for NaB and KCl solutions tested at room temperature. For example, for NaB with a porosity of 0.79 and tested with 9 mM KCl solution at room temperature, Malusis and Shackelford (2002) reported a D^* value for Cl⁻ of 1.2 x 10^{-10} m²/s.

CONCLUSION

A testing apparatus was developed for simultaneous measurement of membrane behavior and diffusion in clays under controlled temperature and chemical conditions. Example results demonstrate the ability of the apparatus to maintain the specimen temperature at 50 °C throughout long-term testing via automated heating regulation and control. For the same 10 mM KCl source solution, the measured value of ω at 50 °C was substantially lower than ω measured at room temperature (58.5 % vs. 19.1 %). Surprisingly, the D^* values were similar for the two temperatures. The complex relationship between temperature and solute transport properties ω and D^* are the focus of an ongoing study utilizing the apparatus described herein. The results of the research have important implications for rates of contaminant transport occurring across bentonite barriers under elevated temperature conditions.

ACKNOWLEDGEMENTS

Financial support for this project is provided by the U.S. National Science Foundation (NSF), Arlington, VA under Grant No. CMMI-1812550. The opinions expressed in this paper are solely those of the authors and are not necessarily consistent with the policies or opinions of the NSF.

REFERENCES

- Cho, W. J., Lee, J. O., and Chun, K. S. (1999). "The temperature effects on hydraulic conductivity of compacted bentonite." *Applied Clay Science*, 14(1–3), 47–58.
- Daniels, K., Harrington, J., Zihms, S., and Wiseall, A. (2017). "Bentonite Permeability at Elevated Temperature." *Geosciences*, 7(1), 3.
- Dominijanni, A., Manassero, M., and Puma, S. (2013). "Coupled chemical-hydraulic-mechanical behaviour of bentonites." *Géotechnique*, 63(3), 191–205.
- Eriksen, T., Jacobsson, A., and Pusch, R. (1981). "Ion diffusion through highly compacted bentonite." KBS TR 81-06, Swedish Nuclear Fuel and Waste Management Co., Stockholm, Sweden.
- Fox, P. M., Tinnacher, R. M., Cheshire, M. C., Caporuscio, F., Carrero, S., and Nico, P. S. (2019). "Effects of bentonite heating on U(VI) adsorption." *Applied Geochemistry*, 109, 104392.
- François, B., and Ettahiri, S. (2012). "Role of the Soil Mineralogy on the Temperature Dependence of the Water Retention Curve." *Unsaturated Soils: Research and Applications*, C. Mancuso, C. Jommi, and F. D'Onza, eds., Springer Berlin Heidelberg, Berlin, Heidelberg, 173–178.
- Gray, M. (1993). "OECD/NEA International Stripa project 1980-1992. Overview volume 3, Engineered Barriers, SKB, Stockholm, Sweden.
- Hao, Z., Sun, M., Ducoste, J. J., Benson, C. H., Luettich, S., Castaldi, M. J., and Barlaz, M. A. (2017). "Heat Generation and Accumulation in Municipal Solid Waste Landfills." *Environmental Science & Technology*, 51(21), 12434–12442.

- Johnson, L., Niemeyer, M., Klubertanz, G., Siegel, P., Gribi, P., (2002). "Calculations of the temperature evolution of a repository for spent fuel, vitrified high-level waste and intermediate level waste in Opalinus Clay." NAGRA Technical Report 01-04, Switzerland.
- Kang, J. B. and Shackelford, C. D. (2010). "Membrane behavior of compacted clay liners." *Journal of Geotechnical and Geoenvironmental Engineering*, 136(10), 1368-1382.
- Kozaki, T., Sato, H., Sato, S., and Ohashi, H. (1999). "Diffusion mechanism of cesium ions in compacted montmorillonite." *Engineering Geology*, 54(1-2), 223-230.
- Lake, C. and Rowe, R. (2000). "Diffusion of sodium and chloride through geosynthetic clay liners." *Geotextiles and Geomembranes*, 18(2-4), 103–131.
- Malusis, M. A., Shackelford, C. D., and Olsen, H. W. (2001). "A laboratory apparatus to measure chemico-osmotic efficiency coefficients for clay soils." *Geotechnical Testing Journal*, 24(3), 229–242.
- Malusis, M. A. and Shackelford, C. D. (2002). "Coupling effects during steady-state solute diffusion through a semipermeable clay membrane." *Environmental Science & Technology*, 36(6), 1312–1319.
- OECD Nuclear Energy Agency and European Commission (Eds.). (2004). Engineered barrier systems (EBS): Design requirements and constraints; Workshop Proceedings, Turku, Finland, 26-29 August 2003, Issy-les-Moulineaux, France.
- Pusch, R. (2001). "The buffer and backfill handbook. part 2: materials and techniques." *Report no. TR-02-12*, Swedish Nuclear Fuel and Waste Management Co.
- Pusch, R., Börgesson, L., and Ramqvist, G. (1985). "Final report of the buffer mass test Volume 2: Test results, Stripa Project Technical Report TR 87-29, SKB, Stockholm, Sweden.
- Rowe, R. K., Caers, C. J., and Barone, F. (1988). "Laboratory determination of diffusion and distribution coefficients of contaminants using undisturbed clayey soil." *Canadian Geotechnical Journal*, 25(1), 108-1185.
- Shackelford, C. D. (1991). "Laboratory diffusion testing for waste disposal A review." *Journal of Contaminant Hydrology*, 7(3), 177–217.
- Shackelford, C. (2013). "Membrane behavior in engineered bentonite-based containment barriers: State of the art." *Coupled Phenomena in Environmental Geotechnics*, M. Manassero, A. Dominijanni, S. Foti, and G. Musso, Eds., July 1-32013, Torino, Italy, CRC Press/Balkema, Taylor & Francis Group, London: 45-60.
- Shackelford, C. D. (2014). "The ISSMGE Kerry Rowe Lecture: The role of diffusion in environmental geotechnics." *Canadian Geotechnical Journal*, 51(11), 1219–1242.
- Shackelford, C. D., Benson, C. H., Katsumi, T., Edil, T. & Lin, L. (2000). "Evaluating the hydraulic conductivity of GCLs permeated with non-standard liquids." *Geotextiles and Geomembranes*, 18(2–4), 133–161.
- Sokolov, V. N and Tchistiakov, A. A. (1999). "Physico-chemical factors of clay particle stability and transport in sandstone porous media." *Proceedings of European Geothermal Conference*, Basel, Switzerland, September 28-30, 1999, Vol. 2, 199-209.
- Wersin, P., Johnson, L., and McKinley, I. (2007). "Performance of the bentonite barrier at temperatures beyond 100°C: A critical review." *Physics and Chemistry of the Earth, Parts A/B/C*, 32(8–14), 780–788.
- Yafrate, N., and Luettich, S. (2017). "Elevated temperature landfills." EM Magazine, May 2017.
- Zheng, L., Rutqvist, J., Birkholzer, J. T., and Liu, H.-H. (2015). "On the impact of temperatures up to 200 °C in clay repositories with bentonite engineer barrier systems: A study with coupled thermal, hydrological, chemical, and mechanical modeling." *Engineering Geology*, 197, 278–295.
- Zihms, S. G., and Harrington, J. F. (2015). "Thermal cycling: impact on bentonite permeability." *Mineralogical Magazine*, 79(6), 1543–1550.